Article

Protective role of Kv7 channels in oxygen and glucose deprivation-induced damage in rat caudate brain slices

Barrese, Vincenzo, Taglialatela, Maurizio, Greenwood, Iain A and Davidson, Colin

Barrese, Vincenzo, Taglialatela, Maurizio, Greenwood, Iain A and Davidson, Colin (2015) Protective role of Kv7 channels in oxygen and glucose deprivation-induced damage in rat caudate brain slices. Journal of Cerebral Blood Flow & Metabolism, 35 (10). pp. 1593-1600. ISSN 0271-678X

PROTECTIVE ROLE OF K_V7 CHANNELS IN OXYGEN AND GLUCOSE DEPRIVATION-INDUCED DAMAGE IN CAUDATE BRAIN SLICES

Vincenzo Barrese PhD[1,2] , Maurizio Taglialatela PhD[2,3], Iain A Greenwood PhD[1] and Colin Davidson PhD[1*]

[1]Division of Biomedical Sciences, St George's University of London, London SW17 0RE, UK;

[2]Neuroscience Reproductive Sciences and Odontostomatology, University of Naples Federico II, Naples, Italy;

[3]Medicine and Health Science, University of Molise, Campobasso, Italy

*Corresponding author

Colin Davidson

cdavidso@sgul.ac.uk

UK (0)208 266 6135

Running Head: retigabine and stroke

Support:

ABSTRACT

Ischemic stroke can cause dopamine efflux that contributes to cell death. Since K_v7 potassium channels regulate dopamine release, we investigated the effects of their pharmacological modulation on dopamine efflux and neurotoxicity in caudate brain slices undergoing oxygen- and glucose- deprivation (OGD). The K_v7 activators retigabine and ICA27243 delayed the onset, and decreased the peak level of dopamine efflux induced by OGD; and also decreased OGD-induced damage measured by 2,3,5-triphenyltetrazolium chloride (TTC) staining. Retigabine also reduced OGD-induced necrotic cell death evaluated by lactate dehydrogenase activity assay. The K_v7 blocker linopirdine increased OGD-evoked dopamine efflux and OGD-induced damage, and attenuated the effects of retigabine. Quantitative-PCR experiments showed that OGD caused a ~6-fold decrease in $K_v7.2$ transcript, while levels of mRNAs encoding for other K_v7 subunits were unaffected; western blot experiments showed a parallel reduction in $K_v7.2$ protein levels. Retigabine also decreased the peak level of dopamine efflux induced by L-glutamate, and attenuated the loss of TTC staining induced by the excitotoxin. These results suggest a role for $K_v7.2$ in modulating ischemia-evoked caudate damage.

KEYWORDS

Oxygen-glucose deprivation, ischemia, dopamine, K_v7 potassium channels, neuroprotection, voltammetry

INTRODUCTION

Pharmacological treatments for ischemic stroke mostly rely on recombinant tissue plasminogen activator (rt-PA) administration, often showing sub-optimal efficiency[1]. Therefore, new neuroprotective drugs, possibly targeting different mechanisms occurring during ischemic stroke, are needed. In stroke and hypoxia, ATP loss results in failure of membrane transporters and ion channels, with subsequent membrane depolarization and aberrant neurotransmitters efflux, thus amplifying injury[2]. Increased neuronal excitability seems to be a pathogenic mechanism underlying different diseases, such as Alzheimer's disease and epilepsy; moreover, epidemiologic studies as well as experiments on animal models have demonstrated a relationship between ischemia and seizures.[3] Based on these observations, antiepileptic drugs have been also proposed for stroke treatment[4]. Although glutamate release has been viewed as a main cause of neuronal damage, massive release of monoamines, such as dopamine, also occurring immediately following the onset of ischemia, can be neurotoxic and thus contribute to cell death[5]. Moreover, it has been demonstrated that chronic methamphetamine administration, as well as striatal injection of dopamine caused a marked pre- and post-synaptic neuronal death in rodents[6]. Dopamine release during ischemia is supposed to be a consequence of different mechanisms, such as cell depolarization, reversal of dopamine transporters and ATP shortage[7]. Among the various regulators of neurotransmitter release, voltage-gated potassium channels belonging to the K_v7 subfamily have emerged as possible targets for hyper-excitability CNS diseases. The K_v7 family comprises five members; $K_v7.2$-$K_v7.5$ subunits underlie the M current (I_{KM}), a potassium current that reduces neuronal excitability, limiting repetitive neuronal firing[8]. In neurons, I_{KM} is mainly determined by hetero-tetramers comprised of $K_v7.2$ and $K_v7.3$ subunits; mutations in Kv7.2 and Kv7.3 are responsible for inherited and sporadic forms of neonatal-onset epilepsies with wide phenotypic heterogeneity, ranging from Benign Familial Neonatal Seizures to epileptic encephalopathy[9,10,11]. $K_v7.5$ and $K_v7.4$ subunits also contribute to M-current heterogeneity in neurons, but their role is more dominant in non-neuronal tissue, such as inner ear ($K_v7.4$), smooth muscle ($K_v7.4$ and $K_v7.5$)[12]

and skeletal muscle (K_v7.4 and K_v7.5)[8,12]. Pharmacological modulation of the M-current modifies depolarization-induced neurotransmitter release in different brain areas[13]. In particular the K_v7 activator retigabine, a recently marketed anti-epileptic drug used as adjunctive treatment in patients with refractory epilepsy, was able to decrease dopamine release from isolated striatal nerve terminals exposed to high extracellular K^+ concentrations[14]. In addition, while some studies have demonstrated that K_v7 activators reduced neuronal damage in hippocampal brain slices[15,16], others found that M-current activation increased death in hippocampal cultured neurons[17].

The aim of this study was to investigate the potential neuroprotective role of K_v7 channels in an *in vitro* model of ischemia, by evaluating the pharmacological modulation of K_v7 channels on dopamine efflux and on neurotoxicity in rat caudate, a region often damaged in ischemic stroke[18].

MATERIALS AND METHODS

Animals and brain slices. Adult male Wistar rats (8-10 weeks old) were killed by cervical dislocation, in accordance with UK Home Office legislation. The brain was quickly dissected and coronal slices (400 µm thick) at the level of the striatum were cut and maintained in artificial cerebrospinal fluid (aCSF). The composition of aCSF was (mM): NaCl (126.0), KCl (2.0), KH2PO4 (1.4), MgSO4 (2.0), NaHCO3 (26.0), CaCl2 (2.4), (+)-glucose (10.0), bubbled for at least 30 min with 95% O2/5% CO2. Once cut, slices were left to equilibrate for 1–4 h at 21±1 ◦C, to allow recovery from any trauma associated with slicing[7].

Fast Cyclic Voltammetry (FCV). The FCV recording apparatus comprised a slice chamber (approx. 2 ml) with the superfusate heated via a thermostatically controlled circulating water bath (Grant, Cambridgeshire, UK). Brain slices were continuously superfused with aCSF, at 32.5±0.5ºC, with a flow rate of 100 mL/h. We applied a triangular voltage waveform (-1 to +1.4V) to the carbon fibre electrode (7 µm diameter x 50 µm length), with a Ag/AgCl reference electrode[12]; the electrochemical signal from carbon-fibre microelectrode, placed into the dorsolateral caudate, was sampled once per second, digitized and recorded using Spike7 (CED, Cambridge, UK). An increase in the current at +600 mV, (the oxidation peak, see Fig 1 inset) together with a corresponding reduction peak at −200 mV is indicative of dopamine.

FCV data analysis. Analysis of data was performed offline using Spike7. Four parameters were measured: (1) time to onset of dopamine release from the initiation of OGD superfusion (T_{on}); (2) time taken to reach maximum dopamine release after the onset of release (T_{peak}); (3) maximum extracellular dopamine concentration (DA_{peak}); and (4) mean rate of dopamine release (DA/T_{peak}).

Experimental protocol for oxygen- and glucose- deprivation and L-glutamate-induced toxicity. Slices were allowed to equilibrate for 15 min in normal aCSF, to assess that no spontaneous

dopamine release occurred, indicating poor slice health[12], then incubated with aCSF containing 0.1% DMSO or drug for an additional 15 min before exposure to ischemic or excitotoxic insults. To this aim, slices were superfused with oxygen and glucose deprived aCSF (OGD-aCSF, 2mM glucose, continuously bubbled with 95% N_2/5% CO_2) or with 10mM L-Glutamate, respectively. These insults were delivered during continued presence of DMSO or test agent until dopamine release occurred (for FCV experiments) or for 15 min (for TTC staining and LDH assay). For qPCR, western blot, TTC staining experiments and LDH assay, slices were also reperfused for 30-60 min with normal aCSF containing DMSO or drug after OGD, to mimic reperfusion and allow time for cell damage to occur.

TTC staining. Separate slices were stained with 2,3,5-triphenyltetrazolium chloride (TTC) in aCSF (0.125% w/v) at 21±1 ◦C for 30 min and then fixed in 4% paraformaldehyde; photographed and analyzed using ImageJ software (http://rsb.info.nih.gov/ij/). Data analysis was performed independently by two researchers, one of which was blinded to experimental groups.

Real time PCR. Total RNA was extracted from brain slices using the RNeasy Mini kit (Qiagen, U.K.) and reverse transcribed using Moloney Murine Leukemia Virus (M-MLV; Invitrogen, U.K.). Quantitative PCR analysis was performed with the CFX96 machine (Biorad, U.K.), using SYBR green master mix and specific primers (PrimerDesign, Ltd., U.K.), followed by melt curve analysis. No template controls (NTCs) were run alongside all reactions to assess contamination. Cycle threshold (Ct) values were determined and normalized to GAPDH housekeeping gene. Relative abundance of each gene of interest was calculated using the $2^{-\Delta\Delta Ct}$ formula.

Western Blot. Brain slices were homogenized in 100 µL lysis buffer (in mMol/L: 20 Tris base, 137 NaCl, 2 EDTA, 1% NP40, 10% glycerol, pH 8, and 10 µL/mL protease inhibitor cocktail; Sigma-Aldrich), denatured at 95°C for 5 min in the presence of sample buffer and reducing agent (Invitrogen) and loaded onto SDS-PAGE gels (4–12% Bis-Tris, Invitrogen), followed by transfer onto a polyvinylidene fluoride membrane (Amersham Biosciences). The membrane was then probed with an anti-K_v7.2 antibody (dilution 1:500; Millipore). Protein bands were visualized with enhanced

chemiluminescence (Thermo Scientific) and hyperfilm (Amersham Bioscience). The membranes were re-probed for β-actin (1:5000; Sigma-Aldrich, A1978), used as loading control. Bands were quantified with Image J.

LDH assay. Neuronal necrotic damage was assessed by measuring lactate dehydrogenase (LDH) activity in the incubation medium, using a specific kit and following manufacturer's instructions (Abcam, Cambridge, U.K.). Briefly, slices were incubated in 24-well plates and exposed to normal- and OGD-aCSF, in the presence of 0.1% DMSO or drug, as described above. 50 µL of incubation medium were taken at different time point (30 and 60 min of reoxygenation period) and mixed with reaction buffer, in the presence of a substrate for LDH. NADH generated by LDH activity interacted with a specific probe in a colorimetric reaction that can be read at 450 nm in a microplate reader. Each sample was assayed in duplicate in a 96-well plate. Absorbance was measured at time 0 and after 30 min incubation at 37◦C. LDH activity (mU/mL) was calculated by comparing samples OD values to those obtained from known NADH standards. Values were then normalized to protein concentration and results are shown as percentage of control slices.

Drugs. Several drugs with specificity for different K_v7 channel subtypes were tested, in particular: i) the pan-K_v7 activator retigabine), opening $K_v7.2$ and $K_v7.3$ channels at low concentration (<1 µM); ii) ICA27243 , a $K_v7.2/K_v7.3$-preferring activator, showing 20- to 100-fold lower potency on $K_v7.4$ and $K_v7.5$; iii) NS15370, a retigabine-analogue able to activate all K_v7 subunits at sub-micromolar concentrations. All activators were a kind gift from Prof SP Olesen (Biomedical Sciences Institute, University of Copenhagen). The Kv7 blockers XE991 and linopirdine as well as the dopamine D1 receptor antagonist SCH23390 were from Tocris Bioscience (Cambridge, U.K.). The dopamine D2 receptor antagonist metoclopramide and L-glutamate were from Sigma-Aldrich.

Statistics. Data were compared by use of Student's t tests or one-way ANOVA, with Dunnett's post-hoc correction for multiple comparisons. Significance was set at $p < 0.05$. Values shown are mean ± S.E.M. Authors were not blind to treatment groups.

RESULTS

OGD-evoked dopamine efflux. Exposure of striatal slices to OGD evoked dopamine efflux after 715 ± 36 s (time to onset, T_{on}). Peak dopamine efflux (DA_{peak}) was 7.2 ± 0.9 µM and time to peak dopamine efflux from the onset of dopamine efflux (T_{peak}) was 125 ± 12 s. The average rate of dopamine efflux (DA/T_{peak}) in control slices was 0.11 ± 0.04 µM/s (Fig 1A). The Kv7 activator retigabine (1 µM) delayed the onset of dopamine efflux by about 30% and also reduced dopamine peak and the rate of change of dopamine efflux by about 40 and 60%, respectively (Fig 1B, black columns). ICA27243 (1 µM), a Kv7.2/Kv7.3-preferring activator, reduced dopamine peak by ~60% but it did not significantly affect T_{on}. ICA27243 also reduced T_{peak} by ~60%, although dopamine efflux rate was unaffected (Fig 1B, white columns). In contrast NS15370 (0.1 µM), a more potent Kv7 opener with respect to retigabine doubled the time to reach dopamine peak, reduced the rate of dopamine efflux by ~55%, but did not significantly modify T_{on} or T_{peak} (Fig 1B, grey columns). We then tested two different pan-K_v7 blockers, XE991 and linopirdine (Fig 1C). While 10 µM XE991 did not interfere with OGD-evoked dopamine efflux (Fig 1C, black columns), linopirdine at 10 µM evoked a 4-fold increase in peak dopamine and rate of dopamine efflux when compared to controls (Fig 1C, white columns). Moreover, linopirdine prevented the changes in T_{on}, DA_{peak} and DA/T_{peak} induced by retigabine after OGD superfusion (Fig 1D, white columns).

TTC staining. To further investigate whether K_v7 activators decreased OGD-induced damage, we performed TTC staining experiments on brain slices (Fig 2). Retigabine (0.3-10 µM; Fig 2A) and ICA27243 (0.1-10 µM; Fig 2B) attenuated the loss of TTC staining in slices exposed to OGD. In contrast, exposure of slices to linopirdine (30 µM) enhanced OGD-induced loss of TTC staining, (Fig 2C). Co-incubation of linopirdine at 10 µM reversed the reduction in the loss of TTC-staining exerted by 1 µM retigabine (Fig 2D).

To evaluate whether dopamine exerts neurotoxic effects via over-stimulation of dopamine receptors, we tested the effects of SCH23390 or metoclopramide, D1- and a D2- receptor

antagonists respectively on OGD-induced damage. Neither SCH23390 (10 μM) or metoclopramide (1 μM) prevented the loss of TTC staining in slices exposed to OGD, and these drugs failed to attenuate the potentiated neurotoxic effects evoked by linopirdine (30 μM) (Fig 2E-F).

Lactate dehydrogenase activity. To evaluate the possible molecular mechanisms underlying retigabine-induced neuroprotection, we measured lactate dehydrogenase (LDH) activity in the incubation medium of slices exposed to OGD, as an index of cell necrosis. In OGD-exposed slices, LDH activity was increased by ~80% and ~50% compared to control slices after 30 and 60 min of reoxygenation respectively (Fig 3A, white columns); retigabine (1 μM) reduced OGD-induced increase of LDH activity at both time points (Fig 3A, grey columns).

Q-PCR and Western blots. We next evaluated possible changes in K_v7 transcripts expression after OGD. Exposure of striatal slices to OGD followed by incubation in normal aCSF caused a 6-fold decrease in $K_v7.2$-transcripts measured by Q-PCR; instead, mRNAs encoding for other K_v7 subunits were unaffected (Fig 3B). Western blot experiments showed a reduction also in $K_v7.2$ protein levels (Fig 3C).

L-glutamate toxicity. To assess whether Kv7 channel activation might exert neuroprotective actions in a different model of cytotoxicity, we evaluated the effects of retigabine on both dopamine release and cell damage after exposure of brain slices to high concentrations of L-glutamate. Incubation of slices with L-glutamate (10 mM) caused dopamine efflux after 354 ± 40s, reaching peak dopamine efflux (6.6 ± 1.4 μM) after 44 ± 13 s. Co-incubation with retigabine (1 μM) caused a ~3-fold increase in time to peak and reduced DA_{peak} and DA/T_{peak} by ~70% and ~80% respectively, while it did not significantly affect T_{on} (Fig 4A). Moreover, retigabine attenuated the loss of TTC staining in slices exposed to L-glutamate (Fig 4B).

DISCUSSION

Ionic homeostasis is fundamental for excitable cells such as neurons, since alterations in the concentrations of different ionic species are both causes and consequences of different pathological processes (apoptosis, cell shrinkage, proteases activation) and diseases. In particular, K^+ ion imbalance seems to be strictly linked to neuronal dysfunction, also for the pivotal role exerted by this ion species in controlling the resting membrane potential and cell excitability. Indeed, hyper-excitability is a common feature of many diseases such as epilepsy and ischemia; massive neurotransmitters release occurs during brain ischemia, possibly due to damage-induced depolarisation and/or the rising of intracellular Ca^{2+} concentrations[2]. Thus, modulation of K^+ channel activity has been acknowledged as a possible target for neuroprotection. Among the different neurotransmitters, dopamine release has been demonstrated to reach very high levels soon after an ischemic insult in the caudate, and also to contribute to neuronal damage[5]; indeed, depletion of dopaminergic nigro-striatal projections has been demonstrated to reduce ischemic damage[19]. Dopamine and related compound such as L-DOPA and 6-OH-DOPA are considered potent excitotoxic agents, possibly contributing to neurodegeneration in Parkinson's and Huntington's disease[20]. Given the known effect of the antiepileptic drug retigabine in reducing dopamine release[14,21], we have investigated the possibility that the pharmacological activation of K_v7-mediated currents could exert a neuroprotective effect in an in vitro model of ischemia. In particular, we focused on the striatum, a region frequently damaged in ischemic stroke in humans and rodent models of stroke, such as middle cerebral artery occlusion. In our experiments the K_v7 activator retigabine was able to reduce the peak dopamine efflux and to delay OGD-evoked dopamine efflux. These effects occurred at a retigabine concentration (1 μM) close to the EC_{50} for activation of $K_v7.2/K_v7.3$ heteromers underlying M-current[8], and to the plasma concentrations achieved in vivo in humans[22]. Because these aberrant dopamine concentrations have been shown to be neurotoxic, reductions in the peak dopamine efflux or the rate of dopamine efflux can be considered neuroprotective, as also suggested by TTC staining experiments. This view was corroborated by the results of FCV and TTC experiments using

ICA27243, a compound with higher selectivity at $K_v7.2/K_v7.3$ heterotetramers. In addition NS15370 reduced the time to reach dopamine peak, but did not reproduce the same effects on OGD-evoked dopamine efflux obtained with retigabine and ICA27243. However, it should be mentioned that NS15370 has a very complex pharmacological profile, showing also K_v7 channel blockade at depolarized potentials[23], a characteristic that might in part explain the lack of effects on dopamine efflux. Blockade of K_v7 channels by linopirdine increased the amplitude and hastened the rate of OGD-evoked dopamine efflux; this result was paralleled by the worsening of OGD-induced brain damage caused by exposure to linopirdine, although at a concentration (30 μM) higher than that able to increase OGD-evoked dopamine efflux. Moreover, linopirdine 10 μM was able to reverse the changes in dopamine efflux induced by retigabine, as well as the reduction in TTC staining loss induced by the K_v7 activator. In particular, linopirdine prevented the effect on T-on exerted by retigabine, although it did not modify this parameter when incubated alone, thus arguing in favour of a specific involvement of the M-current. By contrast, the linopirdine-analogue XE-991 (10 μM) did not modulate OGD-evoked dopamine efflux, although it was previously demonstrated that it increased depolarization-induced dopamine efflux from isolated striatal synaptosomes[14] and from striatal brain slices[21]. Differences in the experimental models (isolated terminals/chopped slices versus brain slices), as well as in the experimental procedures (KCl- vs OGD-evoked release, pre-incubation with dopamine re-uptake inhibitors) might explain this discrepancy.

Despite the well-known neurotoxic effects prompted by high levels of dopamine, the molecular mechanisms underlying these actions are not fully understood. Aberrant dopamine levels can induce damage through the formation of oxidative metabolites, derived from both spontaneous or enzyme mediated dopamine oxidation[24,25]. In addition, receptor-mediated mechanisms have been proposed to explain dopamine-induced neurotoxicity and the possible neuroprotective effects of dopamine D1 and D2 receptor antagonists have been investigated in several studies[26]. In our TTC staining experiments, both SCH23390 (D1 receptor antagonist) and metoclopramide (D2 receptor antagonist) failed to reduce OGD-induced damage and did not revert the enhanced toxicity caused by

linopirdine, suggesting that, in our model, brain damage occurred in a dopamine receptor-independent manner. These results are not surprising, since conflicting evidence are present in the literature; indeed, while some studies failed to demonstrate neuroprotection by D1 and or D2 receptor antagonists, others found that receptor stimulation (mainly the D2 subtype) reduced neuronal damage by blocking the apoptotic pathway (for a comprehensive review, see ref 27).

The neuroprotective action of Kv7 channel activation was confirmed by LDH assay showing that incubation with retigabine reduced necrotic death in brain slices exposed to OGD. We also investigated whether retigabine could affect the apoptotic pathway; unfortunately, in our experimental model, no clear programmed cell death (measured by the evaluation of caspase 3 activation) occurred after OGD, even after 2 hours of reoxygenation (data not shown). However, it should be mentioned that the degree of apoptosis can significantly vary depending on the experimental model and type on insult (duration of OGD and re-oxygenation period), being often undetectable[28]. Moreover, in our experimental model, it was not possible to assess cell damage after long incubation time, as viability of brain slice was significantly reduced also in control conditions.

Both qPCR and western blot data showed a selective decrease in $K_v7.2$ subunit expression after OGD. Although we do not know whether this reduction is only a minor consequence of anoxia, or a main pathogenic mechanism through which OGD exerts its neurotoxic effects, pharmacological data suggest that the activation of channels incorporating $K_v7.2$ subunits might counteract the changes prompted by ischemia and, at least in part, protect from brain damage. In addition, it has been demonstrated that in striatal synaptosomes, selective $K_v7.2$ blockade with a subunit-specific antibody was able to completely abolish the effects of retigabine[14], suggesting a primary role of $K_v7.2$ subunits as the molecular determinant of M-current in this brain area. Moreover, $K_v7.2$ and $K_v7.3$ subunits expression levels can be directly regulated by transcription factors such as Sp1 and Repressor Element 1-Silencing Transcription factor (REST)[29]. Neuronal expression of REST is upregulated in many neuronal pathological conditions, such as cerebral ischemia[30]; thus, the

possibility exists that modulation of $K_v7.2$ expression is a primary mechanism to regulate neuronal behaviour during pathological CNS conditions characterized by hyper-excitability. Previous studies have demonstrated that retigabine was neuroprotective in hippocampal slices, possibly because of its anti-oxidant activity[15,16]. Although different brain regions have been investigated, the efficacy of ICA27243, as well as the reversal of retigabine effects by linopirdine, suggests a neuroprotection mediated by M-current activation. The neuroprotective effects of retigabine are further corroborated by the results of our experiments using a different trigger for brain damage. Indeed, retigabine was able to decrease dopamine release and reduce damage in brain slices exposed to high concentrations of L-glutamate. Since massive release of glutamate occurs during stroke thus determining excitotoxicity, these results highlight Kv7 channels as an exciting target for stroke. Indeed the M-current activates in the range of resting membrane potential, maintaining it below the threshold for sodium current activation, thus limiting repetitive firing after sustained stimulation[8]. Moreover, the M-current can reduce subthreshold excitability, representing a "high-pass filter" for triggers arriving to the axon initial segment, a region particularly important for the integration of stimuli converging to the neuron; interestingly, Kv7.2 channels are robustly expressed in this region of the neuron[31]. In this regard, the M-current seems to be a major determinant of intrinsic neuronal firing characteristics[32,33] and its activation might exert beneficial effects not only at pre-synaptic level (reduction of neurotransmitter release) but also at post-synaptic and axonal level (decreased neuronal excitability). In this scenario, retigabine, by causing a leftward shift in the voltage-dependence of Kv7 channels, facilitates channel opening at more depolarized potentials, thus impeding neuronal depolarization and prevent ischemia-induced hyperexcitability.

During ischemia, lack of oxygen leads the damaged tissue to switch to anaerobic processes, lactic acid production and subsequent acidosis. A decrease in pH has been demonstrated to reduce Kv7.2/Kv7.3-mediated currents[34]; although we did not measure pH in the extracellular fluid or in the brain slices, in similar voltammetric experiments in rodent brain slice changes in pH due to local electrical stimulation of the brain slice have been observed[35]. Nevertheless, the possibility exists

that, due to the continuous perfusion system used, H^+ has largely been washed away and the M-current is artificially up-regulated in our experiments. Lactate has been proposed as a neuroprotective agent, based on the "astrocyte-neuron lactate shuttle hypothesis" suggesting that astrocytes can supply lactate as an alternative, possibly the last, energetic substrate to neurons through monocarboxylate transporters (MCT) during sustained neuronal activity[36]. Moreover, blockade of the lactate transporter exacerbates damage induced by glutamate[37] and exogenous lactate can reduce brain damage in in vitro and in vivo models of ischemia[38]. These data are apparently in contradiction with our hypothesis, as lactate production and subsequent acidosis decreases Kv7 currents, thus suggesting that Kv7 activation should be neurotoxic. However, lactate administration does not seem to modify pH, even at high concentration, in contrast to lactic acid[38,39]. Moreover, endogenous lactate production can be limited by MCT activity which, when saturated, can lead to the accumulation of lactic acid and consequent acidosis. Finally, the evidence concerning the neuroprotective effects of lactate is conflicting, as other studies have found that reducing lactate levels can be neuroprotective and that regional acidosis enhances brain damage[40]. We do not know whether, given the complex functional changes produced by ischemia (involving not only acidosis but lactate production also, see below), the protective effects herein reported for Kv7 activators in an ex-vivo slice model would be more or less pronounced in vivo. However, the idea that increasing Kv7 channel activity can be neuroprotective is further confirmed by research published while this manuscript was under review[41]. The authors found that retigabine and two new Kv7 activators reduced infarct size and functional deficits in two in vivo models of stroke.

Taken together, our data suggest that the M-current activation counteracts the OGD- and glutamate-induced efflux of dopamine and subsequent neurotoxicity. This suggests that, in addition to increasing cerebral blood flow which follows cerebral arteries vasodilation[42], M-current openers might provide direct parenchymal protection. Such a dual mechanism of action might represent a new strategy for neuroprotection in stroke.

DISCLOSURE/CONFLICT OF INTEREST

The authors have no conflict of interest to declare

REFERENCES

1. Bhatia R, Hill MD, Shobha N, Menon B, Bal S, Kochar P et al. Low rates of acute recanalization with intravenous recombinant tissue plasminogen activator in ischemic stroke: real-world experience and a call for action. *Stroke* 2010;41:2254-2258.
2. Doyle KP, Simon RP, Stenzel-Poore MP. Mechanisms of ischemic brain damage. *Neuropharmacology* 2008; 55:310–318.
3. Kadam SD, White AM, Staley KJ, Dudek FE. Continuous electroencephalographic monitoring with radio-telemetry in a rat model of perinatal hypoxia-ischemia reveals progressive post-stroke epilepsy. *J Neurosci* 2010; 30:404-15.
4. Costa C, Martella G, Picconi B, Prosperetti C, Pisani A, Di Filippo M et al. Multiple mechanisms underlying the neuroprotective effects of antiepileptic drugs against in vitro ischemia. *Stroke* 2006; 37:1319-1326
5. Globus, M. Y.-T., R. Busto, W. D. Dietrich, E. Martinez, I.Valdes, and M. D. Ginsberg. 1988. Effect of ischemia on the invivo release of striatal dopamine, glutamate and □-aminobutyricacid studied by intracerebral microdialysis. J. Neurochem.51(5): 1455–1464.
6. Kita T, Saraya T, Konishi N, Matsunari Y, Shimada K, Nakamura M, O'Hara K, Wagner GC, Nakashima T. 1-Methyl-4-phenyl-1,2,3,6-tetrahydropyridine pretreatment attenuates methamphetamine-induced dopamine toxicity. *Pharmacol Toxicol* 2003; 92:71-80.
7. Toner CC, Stamford JA. Effects of metabolic alterations on dopamine release in an in vitro model of neostriatal ischaemia. *Brain Res Bull*. 1999; 48:395-9.
8. Soldovieri MV, Miceli F, Taglialatela M. Driving with no brakes: molecular pathophysiology of Kv7 potassium channels. *Physiology (Bethesda)* 2011; 26:365-376.
9. Biervert C. Schroeder BC, Kubisch C, Berkovic SF, Propping P, Jentsch TJ, Steinlein OK. A potassium channel mutation in neonatal human epilepsy. *Science* 1998; 279: 403-406

10. Charlier C, Singh NA, Ryan SG, Lewis TB, Reus BE, Leach RJ, Leppert M. A pore mutation in a novel KQT-like potassium channel gene in an idiopathic epilepsy family. *Nat Genet* 1998; 18:53-5
11. Weckhuysen S, Mandelstam S, Suls A, Audenaert D, Deconinck T, Claes LR, Deprez L, Smets K, Hristova D, Yordanova I, Jordanova A, Ceulemans B, Jansen A, Hasaerts D, Roelens F, Lagae L, Yendle S, Stanley T, Heron SE, Mulley JC, Berkovic SF, Scheffer IE, de Jonghe P. KCNQ2 encephalopathy: emerging phenotype of a neonatal epileptic encephalopathy. *Ann Neurol*. 2012; 71:15-25
12. Stott JB, Jepps TA, Greenwood IA. K(V)7 potassium channels: a new therapeutic target in smooth muscle disorders. *Drug Discov Today* 2014; 19:413-424.
13. Martire M, Castaldo P, D'Amico M, Preziosi P, Annunziato L, Taglialatela M. M channels containing KCNQ2 subunits modulate norepinephrine, aspartate, and GABA release from hippocampal nerve terminals. *J Neurosci* 2004; 24: 592–597
14. Martire M, D'Amico M, Panza E, Miceli F, Viggiano D, Lavergata F et al. Involvement of KCNQ2 subunits in [3H]dopamine release triggered by depolarization and pre-synaptic muscarinic receptor activation from rat striatal synaptosomes. *J Neurochem* 2007; 102:179-193
15. Boscia F, Annunziato L, Taglialatela M. Retigabine and flupirtine exert neuroprotective actions in organotypic hippocampal cultures. *Neuropharmacology* 2006; 51:283-294
16. Gamper N, Zaika O, Li Y, Martin P, Hernandez CC, Perez MR et al. Oxidative modification of M-type K(+) channels as a mechanism of cytoprotective neuronal silencing. *EMBO J* 2006; 25:4996-5004
17. Zhou X, Wei J, Song M, Francis K, Yu SP. Novel role of KCNQ2/3 channels in regulating neuronal cell viability. *Cell Death Differ* 2011; 18:493-505

18. Nys GMS, van Zandvoort MJE, van der Worp HB, Kapelle LJ, de Haan EHF. Neuropsychological and neuroanatomical correlates of perseverative responses in subacute stroke. *Brain* 2006;129: 2148-57.

19. Globus, M. Y.-T., M. D. Ginsberg, W. D. Dietrich, R. Busto, and P. Scheinberg. 1987. Substantia nigra lesion protects against ischemic damage in the striatum. Neurosci. Lett. 80: 251–256.

20. Olney JW, Zorumski CF, Stewart GR, Price MT, Wang GJ, Labruyere J. Excitotoxicity of L-dopa and 6-OH-dopa: implications for Parkinson's and Huntington's diseases. *Exp Neurol* 1990;108:269-272.

21. Jensen MM, Lange SC, Thomsen MS, Hansen HH, Mikkelsen JD. The pharmacological effect of positive KCNQ (Kv7) modulators on dopamine release from striatal slices. *Basic Clin Pharmacol Toxicol* 2011; 109:339-342.

22. Large CH, Sokal DM, Nehlig A, Gunthorpe MJ, Sankar R, Crean CS, Vanlandingham KE, White HS. The spectrum of anticonvulsant efficacy of retigabine (ezogabine) in animal models: implications for clinical use. *Epilepsia* 2012; 53:425-436

23. Dalby-Brown W, Jessen C, Hougaard C, Jensen ML, Jacobsen TA, Nielsen KS et al. Characterization of a novel high-potency positive modulator of K(v)7 channels. *Eur J Pharmacol* 2013; 709:52-63.

24. Graham DG, Tiffany SM, Bell WR Jr, Gutknecht WF. Autoxidation versus covalent binding of quinones as the mechanism of toxicity of dopamine, 6-hydroxydopamine, and related compounds toward C1300 neuroblastoma cells in vitro. *Mol Pharmacol* 1978; 14:644-653.

25. Hastings TG. Enzymatic oxidation of dopamine: the role of prostaglandin H synthase. *J Neurochem* 1995;64:919-924

26. Davis S, Brotchie J, Davies I. Protection of striatal neurons by joint blockade of D1 and D2 receptor subtypes in an in vitro model of cerebral hypoxia. *Exp Neurol* 2002;176:229-236.

27. Bozzi Y, Borrelli E. Dopamine in neurotoxicity and neuroprotection: what do D2 receptors have to do with it? *Trends Neurosci* 2006; 29:167-174..
28. Jones PA, May GR, McLuckie JA, Iwashita A, Sharkey J. Apoptosis is not an invariable component of in vitro models of cortical cerebral ischaemia. *Cell Res* 2004; 14:241-50.
29. Mucha M, Ooi L, Linley JE, Mordaka P, Dalle C, Robertson B et al. Transcriptional control of KCNQ channel genes and the regulation of neuronal excitability. *J Neurosci* 2010; 30:13235-13245.
30. Calderone A, Jover T, Noh KM, Tanaka H, Yokota H, Lin Y et al. Ischemic insults depress the gene silencer REST in neurons destined to die. *J Neurosci* 2003; 23:2112–2121.
31. Pan Z, Kao T, Horvath Z, Lemos J, Sul JY, Cranstoun SD, Bennett V, Scherer SS, Cooper EC. A common ankyrin-G-based mechanism retains KCNQ and NaV channels at electrically active domains of the axon. *J Neurosci* 2006; 26:2599-2613.
32. Prescott SA, Ratté S, De Koninck Y, Sejnowski TJ. Nonlinear interaction between shunting and adaptation controls a switch between integration and coincidence detection in pyramidal neurons. *J Neurosci* 2006; 26:9084-9097.
33. Gunthorpe MJ, Large CH, Sankar R. The mechanism of action of retigabine (ezogabine), a first-in-class K+ channel opener for the treatment of epilepsy. *Epilepsia* 2012; 53:412-424.
34. Prole DL, Marrion NV. Ionic permeation and conduction properties of neuronal KCNQ2/KCNQ3 potassium channels. *Biophys J*. 2004; 86:1454-1469.
35. Heien ML, Johnson MA, Wightman RM. Resolving neurotransmitters detected by fast cyclic voltammetry. *Analytical Chemistry* 2004; 76:5697-5704.
36. Pellerin L, Magistretti PJ. Glutamate uptake into astrocytes stimulates aerobic glycolysis: a mechanism coupling neuronal activity to glucose utilization. *Proc Natl Acad Sci U S A* 1994; 91:10625-10629.
37. Schurr A, Miller JJ, Payne RS, Rigor BM. An increase in lactate output by brain tissue serves to meet the energy needs of glutamate-activated neurons. *J Neurosci* 1999; 19:34-39.

38. Berthet C, Lei H, Thevenet J, Gruetter R, Magistretti PJ, Hirt L. Neuroprotective role of lactate after cerebral ischemia. *J Cereb Blood Flow Metab* 2009; 29:1780-1789.
39. Morishima T, Aoyama M, Iida Y, Yamamoto N, Hirate H, Arima H, Fujita Y, Sasano H, Tsuda T, Katsuya H, Asai K, Sobue K. Lactic acid increases aquaporin 4 expression on the cell membrane of cultured rat astrocytes. *Neurosci Res*. 2008; 61:18-26.
40. Geng X, Sy CA, Kwiecien TD, Ji X, Peng C, Rastogi R, Cai L, Du H, Brogan D, Singh S, Rafols JA, Ding Y. Reduced cerebral monocarboxylate transporters and lactate levels by ethanol and normobaric oxygen therapy in severe transient and permanent ischemic stroke. Brain Res. 2015; S0006-8993(15)00060-8
41. Bierbower SM, Choveau FS, Lechleiter JD, Shapiro MS. Augmentation of M-Type (KCNQ) Potassium Channels as a Novel Strategy to Reduce Stroke-Induced Brain Injury. *J Neurosci* 2015; 35:2101-2111.
42. Zhong XZ, Harhun MI, Olesen SP, Ohya S, Moffatt JD, Cole WC et al. Participation of KCNQ (Kv7) potassium channels in myogenic control of cerebral arterial diameter. *J Physiol* 2010; 588:3277-3293

TITLES AND LEGENDS TO FIGURES

FIGURE 1. Effects of K_v7-acting drugs on OGD-induced dopamine efflux. **(A)** Representative experiments showing dopamine efflux elicited by OGD in the presence of vehicle (top trace) and 1 μM retigabine (bottom trace); the arrow indicate the onset of dopamine efflux. The inset shows the cyclic voltammogram obtained by plotting the faradaic current against the input voltage. Faradaic currents are obtained by subtracting the signal recorded at the carbon fiber electrode in the absence of dopamine from the signal in the presence of dopamine. Peaks due to the oxidation (OX) and reduction (RED) of dopamine are indicated. **(B-C)** Effects of Kv7 activators (B: retigabine, ICA27243 and NS15370), and blockers (C: XE-991 and linopirdine) on time to onset, time to peak, maximum extracellular dopamine concentration and mean rate of dopamine efflux. **(D)** Effects of 1 μM retigabine alone (black columns) or co-incubated with 10 μM linopirdine (white columns) on dopamine efflux parameters. Data are expressed as percentage of DMSO-treated slices (controls, represented by the dashed line). Values are mean ± S.E.M of 5-9 slices from 5-6 rats. *$p < 0.05$

FIGURE 2. Effects of K_v7-acting drugs and dopamine receptor antagonists on OGD-induced toxicity measured by TTC staining. (A-C) Effects on TTC staining exerted by increasing concentrations of retigabine (A), ICA27243 (B) and linopirdine (C) in OGD-exposed brain slices, as indicated. Data from vehicle treated slices are represented with white columns. **(D)** Effects on TTC staining of 1μM retigabine alone (white columns) or co-incubated with 10μM linopirdine (light grey columns). **(E-F)** Effects on TTC staining in OGD-exposed slices of 10 μM SCH23390 (E) and 1 μM metoclopramide (F) used alone and co-incubated with 30 μM linopirdine**.** Data from vehicle treated slices are represented with white columns. All data are expressed as percentage of normal aCSF-incubated slices (control, black columns). Each bar represents the mean ± S.E.M of 4-7 slices from 4-5 rats. *$p < 0.05$.

FIGURE 3. Effects of retigabine on OGD-induced necrosis and effects of OGD on K_v7 subunits expression (A) Bar graph showing LDH activity measured in the incubation medium in brain slices exposed to normal aCSF (control, black columns), to OGD+vehicle (white columns) or to OGD+1 μM retigabine, after 30 and 60 min of reoxygenation. Data are expressed as percentage of respective control. Each bar represents the mean ± S.E.M. of 8-10 slices from 4-5 rats. *$p < 0.05$. **(B)** Q-PCR experiments showing mRNA levels encoding for K_v7 subunits in striatal slices exposed to normal aCSF (control) or OGD. Data are normalized to housekeeping gene gapdh and expressed as relative to the average of controls, using the $2^{-\Delta\Delta Ct}$ formula. Values are mean ± S.E.M of 4-6 slices. *$p < 0.05$. **(C)** Western blot analysis for $K_v7.2$ protein expression on total lysates from control- or OGD-treated slices. The inset shows a representative blot for $K_v7.2$ and β-actin. The approximate molecular mass for each of these proteins (expressed in kDa) is shown on the left. Bar graph shows the quantification of the averaged OD values for the $K_v7.2$ bands, normalized to the OD value for β-actin, in both normal aCSF (black columns) and OGD-exposed (white columns) slices. *$p < 0.05$ vs. respective control; n=5 for both control- and OGD-exposed slices.

FIGURE 4. Effects of retigabine on L-glutamate-induced dopamine release and toxicity. (A) FCV experiments showing the effects of 1 μM retigabine on time to onset, time to peak, maximum extracellular dopamine concentration and mean rate of dopamine efflux in brain slices exposed to 10 mM L-glutamate. Data are expressed as percentage of DMSO-treated slices (controls, black columns). Values are mean ± S.E.M of 5-9 slices from 5-6 rats. *$p < 0.05$. The inset shows representative experiments of dopamine efflux elicited by OGD in the presence of vehicle (top trace) and 1 μM retigabine (bottom trace); the arrow indicate the onset of dopamine peak. The cyclic voltammogram generated by plotting the faradaic current against the input voltage is also shown. Peaks due to the oxidation (OX) and reduction (RED) of dopamine are indicated. **(B)** Bar graph showing the effects of exposure to 10 mM L-glutamate in the presence of DMSO (white column) or 1 μM retigabine (grey column). Data are expressed as percentage of DMSO-treated slices (control with no L-glutamate, black column). Values are mean ± S.E.M of 6-8 slices from 3-4 rats. *$p < 0.05$.

Fig 1

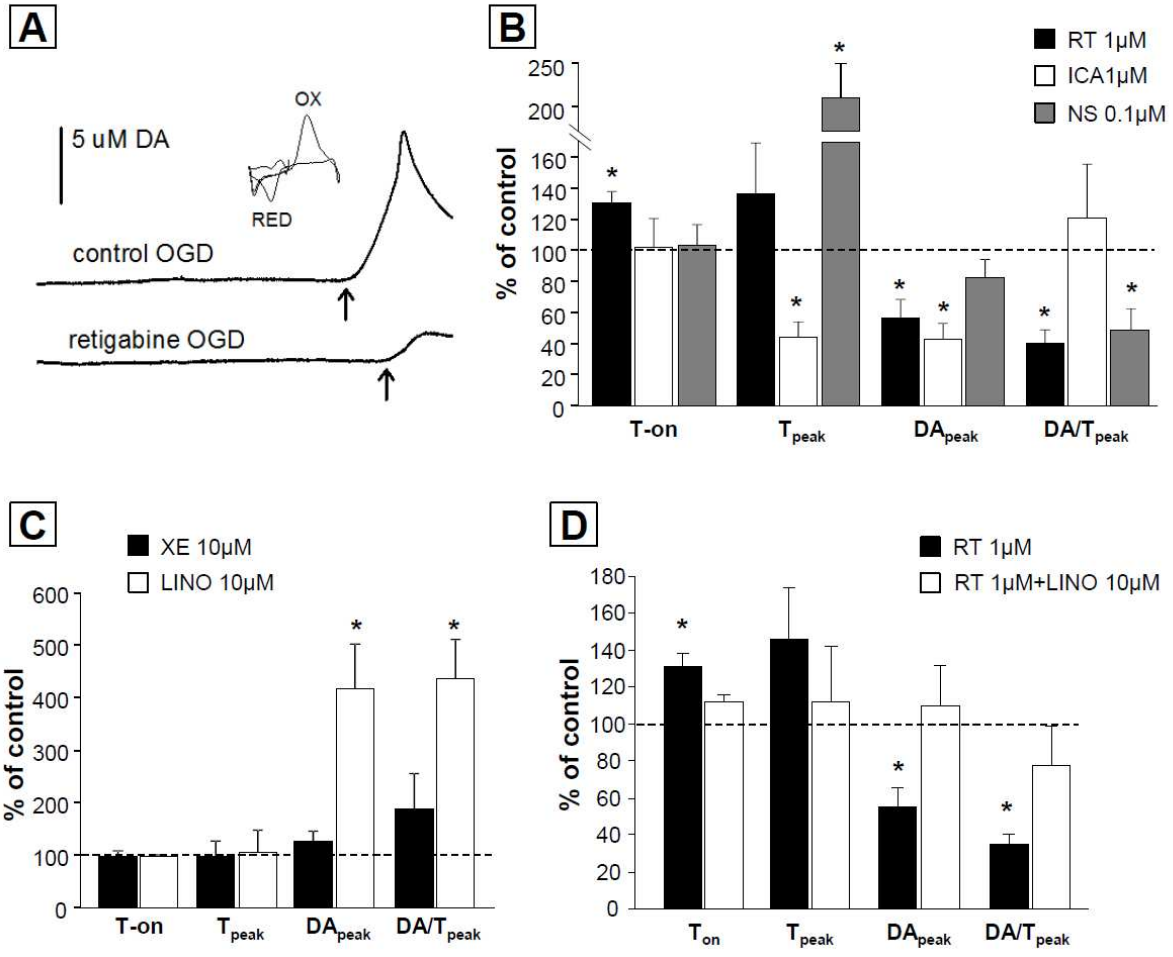
A
5 uM DA
OX
RED
control OGD
retigabine OGD
B
RT 1μM
ICA1μM
NS 0.1μM
% of control
T-on
T peak
DA peak
DA/T peak
C
XE 10μM
LINO 10μM
% of control
T-on
T peak
DA peak
DA/T peak
D
RT 1μM
RT 1μM+LINO 10μM
% of control
T on
T peak
DA peak
DA/T peak

Fig 2

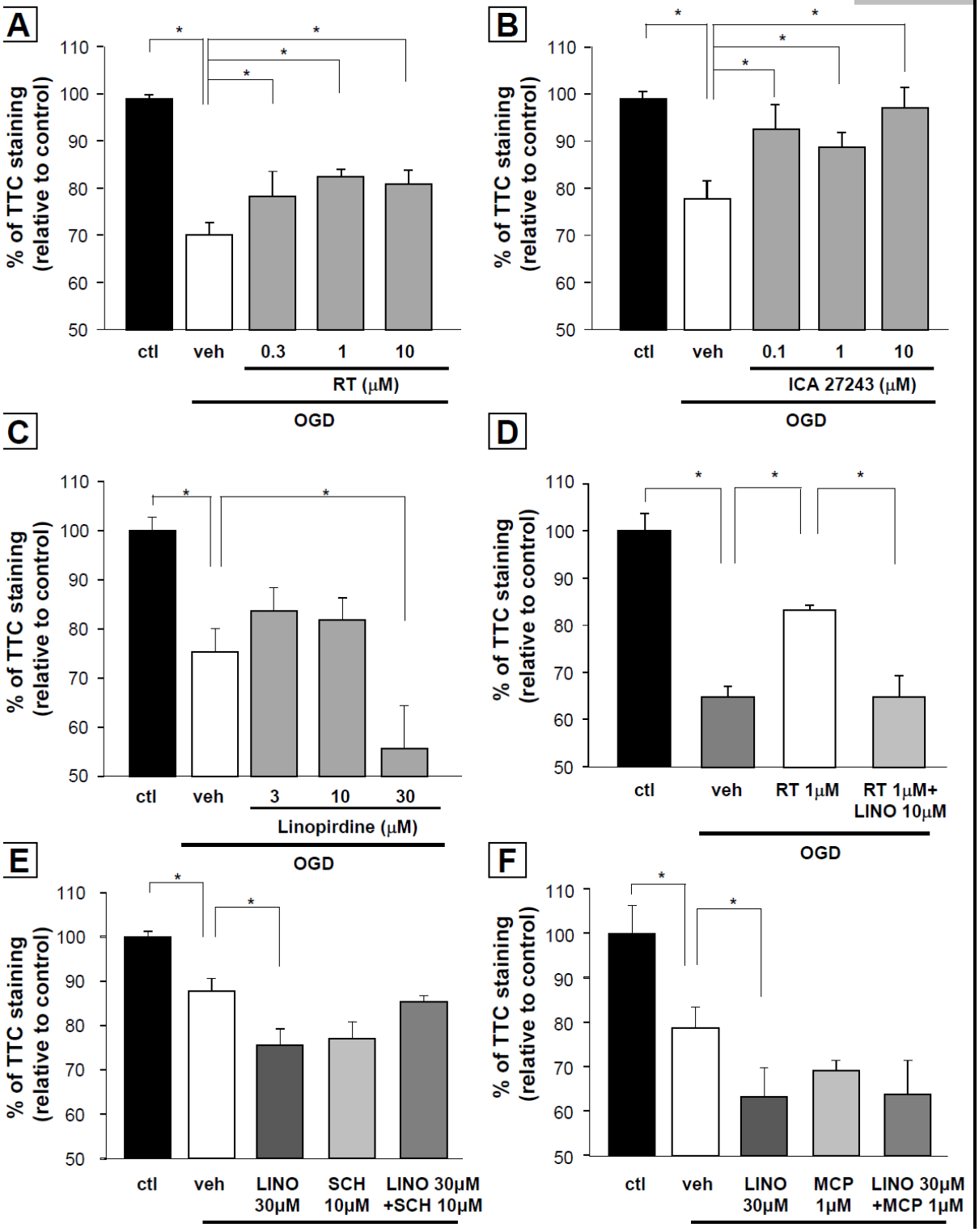
A
% of TTC staining (relative to control)
110
100
90
80
70
60
50
ctl
veh
0.3
1
10
RT (μM)
OGD
B
% of TTC staining (relative to control)
ctl
veh
0.1
1
10
ICA 27243 (μM)
OGD
C
% of TTC staining (relative to control)
ctl
veh
3
10
30
Linopirdine (μM)
OGD
D
% of TTC staining (relative to control)
ctl
veh
RT 1μM
RT 1μM+ LINO 10μM
OGD
E
% of TTC staining (relative to control)
ctl
veh
LINO 30μM
SCH 10μM
LINO 30μM +SCH 10μM
OGD
F
% of TTC staining (relative to control)
ctl
veh
LINO 30μM
MCP 1μM
LINO 30μM +MCP 1μM

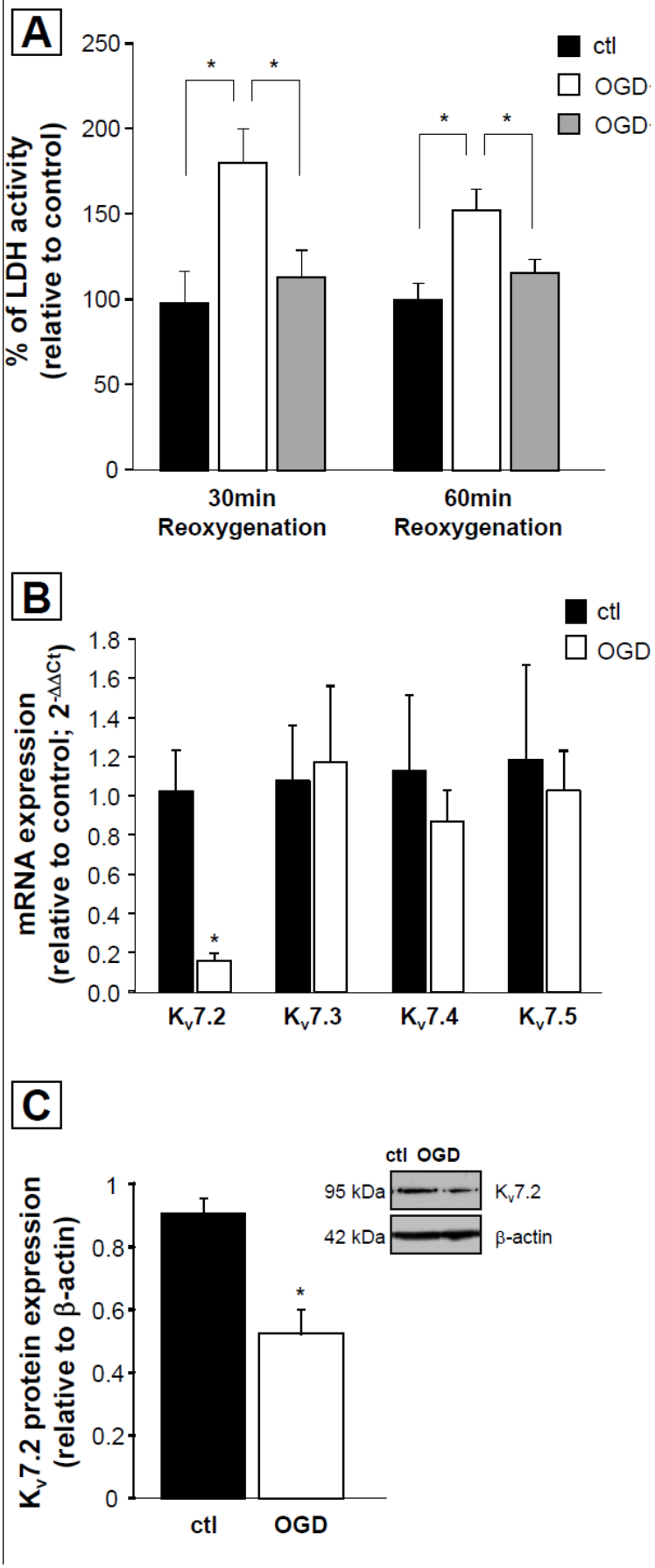
A
% of LDH activity (relative to control)
250
200
150
100
50
0
ctl
OGD
OGD
*
*
*
*
30min Reoxygenation
60min Reoxygenation
B
mRNA expression (relative to control; 2-ΔΔCt)
1.8
1.6
1.4
1.2
1.0
0.8
0.6
0.4
0.2
0.0
ctl
OGD
*
Kv7.2
Kv7.3
Kv7.4
Kv7.5
C
Kv7.2 protein expression (relative to β-actin)
1
0.8
0.6
0.4
0.2
0
ctl OGD
95 kDa
42 kDa
Kv7.2
β-actin
*
ctl
OGD

Fig 4

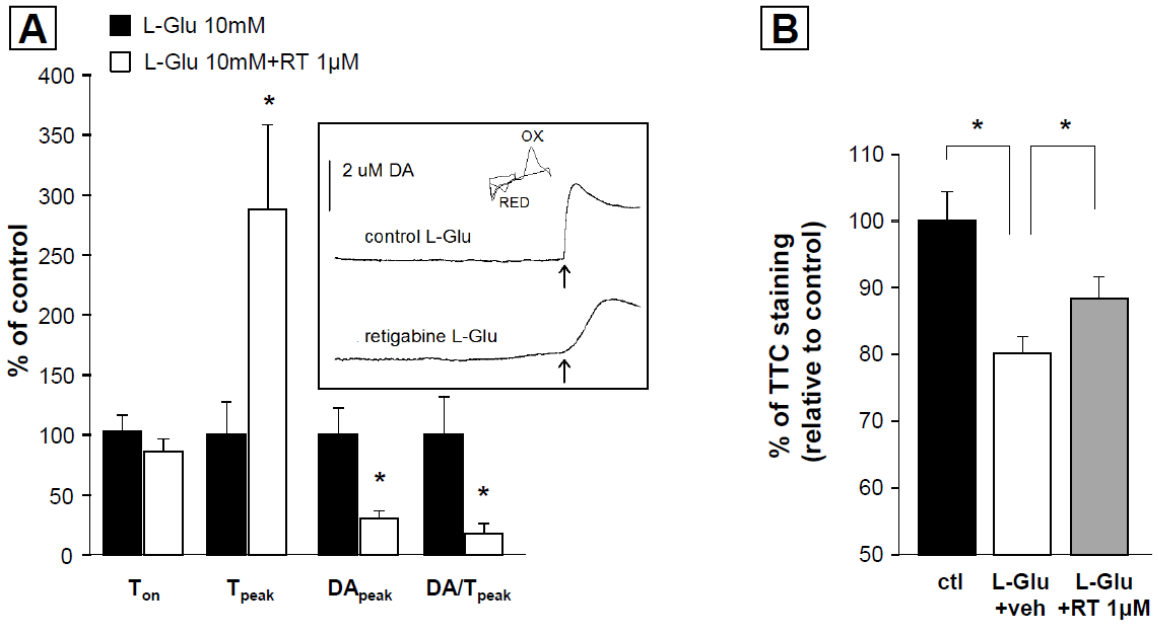
A
L-Glu 10mM
L-Glu 10mM+RT 1µM
% of control
400
350
300
250
200
150
100
50
0
*
*
*
2 uM DA
OX
RED
control L-Glu
retigabine L-Glu
T on
T peak
DA peak
DA/T peak
B
% of TTC staining (relative to control)
110
100
90
80
70
60
50
*
*
ctl
L-Glu +veh
L-Glu +RT 1µM